HEV MODELING FOR A SUPERVISORY LEVEL POWER FLOW CONTROL PROBLEM

Kasemsak Uthaichana[*], Sorin Bengea[**], Raymond DeCarlo[*]

[*]*Purdue University, School of ECE, Northwestern Ave, West Lafayette, IN, 47907, USA*
[**]*Eaton Innovation Center, 15151 Highway 5 Bldg.2, Eden Prairie, MN, 55344, USA*

Abstract: This paper explores the modeling equations underlying a supervisory level power flow control problem for a hybrid electric vehicle (HEV). For a given driving profile, a supervisory controller decides on the power split between the ICE and the battery-electric-motor-generator to achieve optimal performance, e.g., a trade-off between energy usage, driving profile tracking, and drivability constraints. Formulation and solution of such a problem require a supervisory level power flow control model amenable to hybrid optimal control techniques. This paper develops constrained power flow control models for the various HEV subsystems and their interactions, along with a differential equation modeling the HEV's longitudinal dynamics amenable to recent advances in hybrid optimal control theory.

Keywords: hybrid electric vehicles; modeling; power flow control; hybrid optimal control; switching systems; supervisory control.

1. INTRODUCTION

This paper develops a supervisory level power flow control model for a parallel Hybrid Electric Vehicle (HEV). Advantages of the HEV over conventional vehicles are delineated in the literature as are situations where the parallel has advantages over a series configuration (Wouk, 1995; Cuddy and Wipke, 1997, Aylor, *et al.* 1998). Improving the fuel efficiency of such a complex system beyond the limits of rule-based control algorithms is a challenging problem. The consideration of a power-flow-based model is a result of a customary trade-off in control engineering: the model captures the main HEV subsystem's dynamics in a way that renders the model amenable to control techniques.

The HEV utilizes power flow from an internal combustion engine ICE (here 4-cylinders 1.9 L diesel engine) and from an electric-motor battery-pack. A diesel was selected over a gasoline engine for fuel economy; similarly, a continuously variable transmission (CVT) was selected for its potential to enhance the operating efficiency of the ICE as well as a 57 kW electric motor-generator (EM-GEN) primarily because of the availability of data describing its operating efficiency. Emissions are not specifically considered in this paper. The EM-GEN interfaces with an electric battery pack consisting of twenty-seven of 13 Ah 12 V lead acid batteries connected in series. Figure 1 depicts a block diagram of the system of subsystems where arrows indicate (potential) power flows. A companion paper takes up

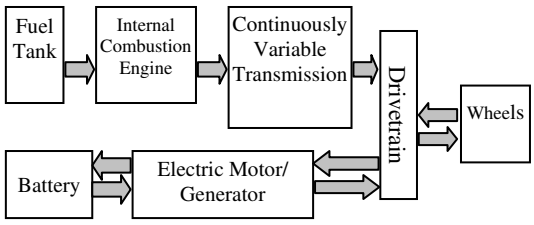

Fig 1. Schematic of HEV power flows.

the details of the associated hybrid optimal control problem (Uthaichana, *et al*., 2005).

The HEV dynamical model detailed in the next section includes a first order differential power equation for the ICE, a differential equation for the state of charge of the battery, a Willan's line representation for the EM-GEN, and a differential equation in the vehicle velocity that is also used to determine the velocity-dependent efficiencies of the subsystems.

The idea of a supervisory level power flow control problem has occurred earlier in Brahma, *et al*., (2000) and C.C. Lin, *et al*., (2003) who adopt a two-level (supervisory and local) hierarchical approach to solving the HEV control problem; their approach uses instantaneous power flow levels, the corresponding efficiencies and/or losses of each subsystem, and the battery SOC in dynamic programming. The conceptual approach taken in this work has elements from both. Yet, in contrast to C.C. Lin, *et al.*, (2003), and whose work used dynamic programming to optimize the fuel economy and emission reduction at the supervisory level, this study strictly solves "power management problem" for the optimal power flow at the supervisory level using vehicle velocity dependent efficiencies. Further, in contrast to Brahma, *et al.* (2000), the power flow modeling is dynamic containing diff. eqs. in engine power, in vehicle velocity, and in SOC, along with velocity dependent efficiencies which add another level of difficulty to the problem. For other related work on HEV modeling and control strategies, see Powell, *et al.* (1998), Paganelli, *et al.*, (2001), Phillips, *et al.*(2000); Saeks, *et al.* (2002).

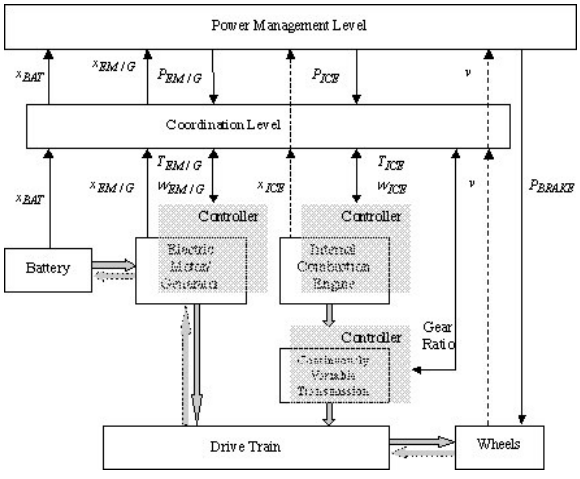

Fig. 2. Supervisory power flow control strategy.

According to C.C. Lin, *et al*., (2003), there are five possible modes of operation for the HEV: motor only, engine only, motor assisted engine, engine charging the battery, and regenerative braking. In the context of the power management perspective taken in this study, the control modes at first appear to be threefold: normal and regenerative braking control, power split control, and battery recharging control. Despite this apparent threesome and other possible subsets of operations, from a strict hybrid systems perspective only two distinct modes of operation are evident: the EM-GEN operates in the motoring mode, denoted EM, or the EM-GEN operates in the generating mode, denoted GEN. We denote the mode of operation by a function $v(t) = 0$ for motoring, and $v(t) = 1$ for generating. Note that the vehicle can be motoring while in the generating mode also.

The sections to follow detail the components of the dynamic power flow model utilized in this work as a switched system with two modes of operation. The modeling details of the important subsystems, i.e., ICE, battery, EM/GEN, brake, and vehicle, are explained successively. In the motoring mode, the only available power sources are the ICE and the EM-battery combination. These devices propel the vehicle through intermediate linkages: the CVT and the drivetrain which transmit power to the vehicle with certain efficiencies/losses that are velocity dependent.

In the generating mode, power is absorbed from the ICE through a coupling and/or from regenerative braking through the drivetrain wherein kinetic energy of the vehicle is stored in the battery. Power absorption by increasing the rotational speed of a fly wheel is not considered here.

2. ICE AND CVT MODELING

2.1 ICE Model

The instantaneous ICE power flow $P_{ICE}(t)$ is quantified at the flywheel[1] and includes losses due to engine pumps, friction, and the valve train. $P_{ICE}(t)$ is assumed unidirectional, i.e., the engine delivers power to the drivetrain and vehicle through a CVT. $P_{ICE}^{des}(t)$ denotes the desired power flow profile computed and demanded by the supervisory control. A first order lag equation captures the dominant power flow dynamics of the ICE:

$$\dot{P}_{ICE}(t) = -\frac{1}{\tau_{ICE}} P_{ICE}(t) + \frac{1}{\tau_{ICE}} P_{ICE}^{des}(t) \quad (1)$$

where τ_{ICE} is the nominal delay associated with the power generation and delivery sequence, i.e., τ_{ICE} can be viewed as the sum of the following: (a) fuel

[1] In certain situations (e.g. regenerative braking, the ICE and its crankshaft is disconnected from the rest of the drivetrain and vehicle. Thus, P_{ICE} is quantified at the flywheel to decouple the effect of crankshaft inertia from the vehicle mass.

injection delay between a fuel command and the actual start of injection, about 40ms; (b) combustion delay or firing delay, which is inversely proportional to the engine speed, $\frac{60 \cdot 2}{4\omega_{ICE}} \in \left[7.5ms,\ 30ms\right]$ corresponding to an engine speed range of 1000 to 4000 rpm; (c) delay of power delivery due to the crankshaft (inertia), about 0.25 s. The sum of (a), (b), and (c) suggests a nominal delay of 0.3 sec. Equation 1 is utilized in both modes of operation. For control purposes we factor

$$P_{ICE}^{des}(t) = P_{ICE}^{\max}(\omega_{ICE}) \cdot u_{ICE}(t) \cdot eng(t) \qquad (2)$$

where (i) $P_{\mathrm{ICE}}^{\max}(\omega)$ is the maximum available ICE power at a given engine speed ω_{ICE}, (ii) $u_{ICE}(t) \in \left[0.2,\ 1\right]$ is a normalized control input that modulates $P_{ICE}^{\max}(\omega_{ICE})$, and (iii) $eng(t) \in \{0,1\}$ is an off-on engine status control used to implement turn-off and turn-on constraints. The lower limit of 0.2 for $u_{ICE}(t)$ is set to limit inefficient engine operation occurring below $0.2P_{ICE}^{\max}(\omega_{ICE})$. At this point we note that $P_{ICE}^{\max}(\omega_{ICE})$ can be related to the efficiency of conversion of fuel to engine power which we reflect appropriately in our performance index so as to minimize a weight on energy/fuel consumption.

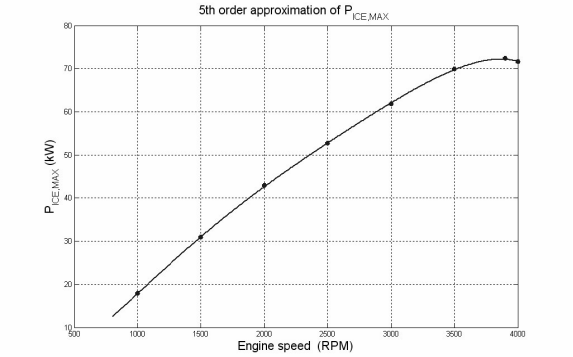

Fig. 3. $P_{ICE}^{\max}(\omega)$ for a 1.9 L diesel engine with superimposed data from Brahma, *et al*., (2000)

Figure 3 shows the $P_{ICE}^{\max}(\omega_{ICE})$ profile heuristically derived from the relationship between maximum torque $T_{ICE}^{\max}$ and engine speed $\omega_{ICE} \in [1000, 4000]$ RPM plotted in Brahma, *et al*., (2000). A 5th order polynomial approximation is given as:

$$P_{ICE}^{\max}\left(\omega_{ICE}\right) = -4.8137\left(\frac{\omega_{ICE}}{10^3}\right)^5 + 51.24\left(\frac{\omega_{ICE}}{10^3}\right)^4 - 206.6\left(\frac{\omega_{ICE}}{10^3}\right)^3 + 366.33\left(\frac{\omega_{ICE}}{10^3}\right)^2 - 35.5\left(\frac{\omega_{ICE}}{10^3}\right) \qquad (3)$$

leading to a 2-norm error of 0.3%. From Fig. 3, $P_{ICE}^{\max}(\omega_{ICE})$ attains its peak power at 3900 RPM. Because the CVT allows for an "infinite" number of possible engine speeds for a given vehicle speed *V(t)*, there is no incentive in this study to achieve a desired ICE power level at speeds beyond 3900 RPM because they can be achieved more efficiently for speeds below this value. For this reason and for a more simplified control problem, we construct a 2nd order polynomial approximation (with a 1.1 % approximation error) for engine speeds between 800 and 3900 RPM:

$$P_{ICE}^{\max}\left(\omega_{ICE}\right) = a_1\left(\frac{\omega_{ICE}}{10^3}\right)^2 + a_2\left(\frac{\omega_{ICE}}{10^3}\right) + a_3 \quad (4)$$

where $a_1 = -3.26$, $a_2 = 35.11$, $a_3 = -14.21$. With the constraint of Eqn. 4 and combining Eqns. 1 and 2, engine power satisfies:

$$\dot{P}_{ICE}(t) = -\frac{1}{\tau_{ICE}} P_{ICE}(t) + \frac{1}{\tau_{ICE}} P_{ICE}^{\max}(\omega_{ICE}) u_{ICE}(t) eng(t) \quad (5)$$

2.2 CVT Model

The ratio of ω_{ICE} to $V(t)$, is given by $k_{v3}G_r$ where k_{v3} is the ratio between the driveshaft and the wheels' radius, and G_r is the gear reduction ratio, which takes values in the interval $G_r \in \left[G_r^{\min}, G_r^{\max}\right] = \left[0.407,\ 2.367\right]$. Thus, the engine speed ranges as,

$$\omega_{ICE} \in \left(\frac{60}{2\pi}\right) k_{v3} V(t) \left[G_r^{\min},\ G_r^{\max}\right] \quad (6)$$

For this study, the vehicle velocity ranges from zero to 20 m/s.

The engine controller modulates the maximum available engine power which depends on ω_{ICE} which in turn depends on $V(t)$ as per Eqn 6 with limiting behaviors indicated in Figure 4: idle speed and redline constraints etc. From Figure 3, $P_{ICE}^{\max}(\omega_{ICE})$ is a monotonically increasing function of $\omega_{ICE} \in \left[\ 800, 3900\ \right]$ which means maximum power corresponds to maximum engine speed, i.e., as per Fig. 4, for each $V(t) \in \left[\ 1.877,\ 20\ \right]$m/s, ω_{ICE} is selected as high as possible, but not more than 3900 RPM in which case $u_{ICE}(t)$ will always modulate the maximum input power to the engine. Also from Fig. 4, for $V(t) < V_{ICE}^{\min} = 1.8377\ (m/s)$, there is no feasible gear ratio and engine speed. For

improved efficiency, the engine may be turned off rather than left to idle. Hence,

$$\omega_{ICE} = \begin{cases} 800 eng(t) & , \quad V \le 1.877 \\ \dfrac{60 k_{v3}}{2\pi} G_r^{\max} V & , \; V \in [1.877, 8.9586] \\ 3900 & , \; V \ge 9.89586 \end{cases} \qquad (7)$$

As per Figure 4, $\omega_{ICE}(V)$ is not differentiable at V = 8.9586 m/s, and must be for the control algorithm. A quadratic polynomial is used to approximate $\omega_{ICE}(V)$ for $V \in [\,8.4586, 9.4586\,]$ making $\omega_{ICE}(V)$ a differentiable function. Thus, with $K_1 = 1.877$, $K_2 = 8.4586$, $K_3 = 9.4586$, $b_1 =$ 435.34 , $b_2 = -217.67$, $b_3 = 4117.7$, and $b_4 =$ -15573.6 :

$$\omega_{ICE}(V) = \begin{cases} 800 eng(t) & V \le K_1 \\ b_1 V & K_1 \le V \le K_2 \\ b_2 V^2 + b_3 V + b_4 & K_2 \le V \le K_3 \\ 3900 & K_3 \le V \le 20 \end{cases} \qquad (8)$$

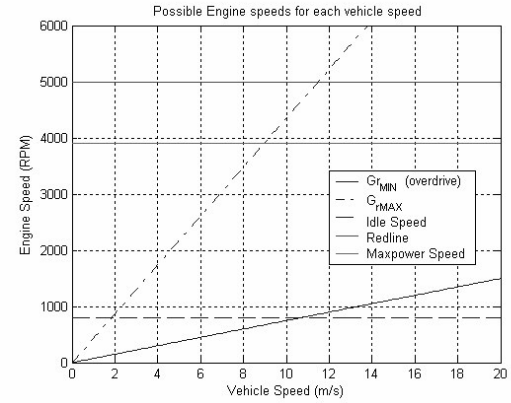

Fig.4. Constrained engine vs. vehicle speed.

At each velocity V , $P_{ICE}^{\max}$ is a composition of the functions $P_{ICE}^{\max}(\omega_{ICE})$ with $\omega_{ICE}(V)$.

3. BATTERY MODELING

The efficiency of the charge-discharge behavior of a battery depends on its state of charge (SOC), i.e., the ratio of instantaneous stored charge to maximum stored charge, and on the power delivered by or delivered to the battery. Hence, the overall energy/fuel efficiency of an HEV requires that the battery pack maintain its SOC between fixed limits that bound its safe high efficiency region of operation, 0.4 to 0.8 for our study. To obtain a usable measure of the SOC, we assume a relatively constant open circuit voltage of the battery during HEV operation. Under this condition, the SOC is approximately give by normalized battery energy, $\bar{W}_{bat}(t) = \dfrac{W_{bat}(t)}{W_{bat}^{\max}}$ where $W_{bat}(t)$ is the instantaneous battery energy, and $W_{bat}^{\max}$ is the maximum rated energy of the battery (Hopka, *et al*., 2000). Thus to maintain proper battery and HEV efficiencies we require that $\bar{W}_{bat}^{\min} = 0.4 \le \bar{W}_{bat} \le \bar{W}_{bat}^{\max} = 0.8$ where $\bar{W}_{bat}^{\min}$ and $\bar{W}_{bat}^{\max}$ are the minimum and maximum operating levels.

The rate at which battery energy is depleted or increased depends on the power ($P_{bat}(t) \ge 0$) delivered, or absorbed ($P_{bat}(t) < 0$). $P_{bat}(t) =$ $P_{loss} + P_{EM/GEN}$ where $P_{loss} = 2$ kW is assumed to be a constant accessory power. $P_{EM,in} = P_{EM/GEN} \ge 0$ means the EM absorbs power and $P_{GEN} = P_{EM/GEN} < 0$ means power is delivered to the battery. Additionally, battery energy depends on the discharge η_{bat}^{mot} and charging efficiencies η_{bat}^{gen} . Since the charge and discharge power flows of the battery energy are controllable, we set $P_{bat}(t) = P_{bat}^{\max} \cdot u_{bat}(t)$ where (i) $P_{bat}^{\max} = \pm 100$ (charging/discharging respectively) is the instantaneous maximum deliverable power at the battery terminal, and (ii) $u_{bat}(t)$ is a normalized control input which modulates $P_{bat}^{\max}$. Further, $u_{bat}(t)$ is constrained as $u_{bat}(t) \in \left[u_{bat}^{\min}, u_{bat}^{\max}\right] \subset [0,1]$. Thus, by differentiating the normalized battery energy and incorporating the above discussion, we have the following differential equation for change in stored energy whose integral approximates the battery SOC:

$$\dot{\bar{W}}_{bat} = -\frac{1}{W_{bat}^{\max}} \eta_{bat}\left(\bar{W}_{bat}, P_{bat}\right) P_{bat} \qquad (9)$$

where $\eta_{bat} = 1/\eta_{bat}^{mot}$ for discharging and $\eta_{bat} = \eta_{bat}^{gen}$ for charging. Equation (9) is nonlinear in P_{bat} which is not amenable to the theoretical development in Bengea and DeCarlo, (2005). Linearizing this equation about a nominal discharging (17 kW) and charging (–18 kW) operating input powers, and observing that $\Delta P_{bat} = P_{bat} - P_{bat,nom}$, we arrive at the following partially linearized equation for SOC:

$$\begin{aligned} \dot{\bar{W}}_{bat} &= \frac{d_{3,v}}{W_{bat}^{\max}} P_{bat,nom}^2 - \Big[\ln\left(d_{1,v}\bar{W}_{bat} + d_{2,v}\right) \\ &\quad + 2 d_{3,v} P_{bat,nom} + d_{4,v}\Big] \frac{P_{bat}^{\max}}{W_{bat}^{\max}} u_{bat}(t) \end{aligned} \qquad (10)$$

with $d_{1,0} = -0.2856$, $d_{2,0} = 1.4734$, $d_{3,0} = 7.569 \cdot 10^{-3}$, $d_{4,0} = 0.6834$, $d_{1,1} = -0.2384$, $d_{2,1} = 1.4852$, $d_{3,1} = 6.872 \cdot 10^{-3}$, and $d_{4,1} = 0.6635$.

The assumption that battery operating efficiency depends both on the power levels drawn from/supplied to the battery, and the (normalized battery energy) SOC is in accord with the discharging and charging efficiency map noted in C.C. Lin, *et al*., (2003) for 25 of 18 Ah 12.5 V lead acid batteries. The expressions of battery efficiency (used in equations 9 and 10) are approximation of the battery profiles in C.C. Lin, *et al*., (2003).

4. THE ELECTRIC MOTOR/GENERATOR

For the perspective of supervisory control, we assume that the EM/GEN dynamics time constants that are much faster than those of the ICE and vehicle. Hence we assume no delay between the EM output power at the motor shaft, $P_{EM}(t)$, and its input power, nor in the generating mode between the generator output, $P_{GEN}(t)$, and its input power. This permits a (algebraic) Willan's line approximation to the EM/GEN. Specifically, in the motoring mode, the EM output power is (in kW)

$$P_{EM/GEM,out} = C_{1v}(\omega_{EM})P_{EM/GEN,in} + \frac{C_{2v}(\omega_{EM})}{1000}\omega_{EM} \quad (11)$$

where (i) ω_{EM} is the EM/GEN shaft velocity, (ii) the Willan's line coefficients are

$$C_{1v}(\omega_{EM}) = \gamma_{11,v}\omega_{EM}^2 + \gamma_{12,v}\omega_{EM} + \gamma_{13,v} \quad (12a)$$

$$C_{2v}(\omega_{EM}) = \gamma_{21,v}\omega_{EM}^2 + \gamma_{22,v}\omega_{EM} + \gamma_{23,v} \quad (12b)$$

with $\gamma_{11,0} = -6.836 \cdot 10^{-7}$, $\gamma_{12,0} = 9.01 \cdot 10^{-4}$, $\gamma_{13,0} = 0.6219$, $\gamma_{21,0} = 9.602 \cdot 10^{-6}$, $\gamma_{22,0} = -9.491 \cdot 10^{-3}$, $\gamma_{23,0} = -1.375$, and $\gamma_{11,1} = -6.0704 \cdot 10^{-7}$, $\gamma_{12,1} = 8.0314 \cdot 10^{-4}$, $\gamma_{13,1} = 0.6465$, $\gamma_{21,1} = -5.9811 \cdot 10^{-6}$, $\gamma_{22,1} = 5.2665 \cdot 10^{-3}$, $\gamma_{23,1} = 1.74$, (iii)

$$P_{EM/GEN,in} = \begin{cases} P_{EM,in} & v = 0 \\ P_{GMec} & v = 1 \end{cases} \quad (13a)$$

and

$$P_{EM/GEN,out} = \begin{cases} P_{EM}(t) & v = 0 \\ P_{GEN}(t) & v = 1 \end{cases} \quad (13b)$$

where P_{GMec} is the mechanical input power to the generator, and (iv) the constraints on the output motoring and generating powers are given in kW with superscript max indicating maximum allowable powers:

$$0 \le P_{EM,out} \le P_{EM}^{\max}(\omega_{EM}) = P_{GEN}^{\max}(\omega_{EM}) \quad (14)$$

$$= \begin{cases} 0.19\omega_{EM} & \omega_{EM} \le 290 \\ \kappa_1\omega_{EM}^2 + \kappa_1\omega_{EM} + \kappa_3 & 290 \le \omega_{EM} \le 310 \\ 57 & \omega_{EM} \ge 310 \end{cases}$$

where $\kappa_1 = -4.75 \cdot 10^{-3}$, $\kappa_2 = 2.945$, and $\kappa_3 = -399.475$.

Finally, the shaft velocity is coupled to the vehicle by the fixed (lock-on) relationship $\omega_{EM} = \lambda_C \cdot k_{v3} \cdot V$ where (i) λ_C is the transmission ratio between the motor speed and the driveshaft speed, ω_C , and (ii) k_{v3} is the ratio between the driveshaft and the wheel radius.

5. COUPLING DEVICE

In each mode, the coupling device (CD) transfers power from its input sources to its output at specific coupling device efficiency, ε_c. In the motoring mode the CD's input power is that of the ICE through the CVT and that of the EM-battery while the output power is expressed by

$$P_C(t) = \varepsilon_c \left[\eta_{tr} P_{ICE}(t) eng(t) + P_{EM}(t)\right] \quad (15)$$

where $\eta_{tr} = 0.95$ is the CVT efficiency. In the generating mode the CD's input power is the ICE through the CVT and the regenerative braking power. The output power is

$$P_{GMec} = \varepsilon_c \left(P_{reg}^{\max} r(t) + split(t)\eta_{tr} P_{ICE}(t) eng(t)\right) \quad (16)$$

where (i) $r(t) \in [0,1]$ represents the control input that is a normalized fraction of the maximum regenerative braking power

$$P_{reg}^{\max}(\omega_{EM}) = \frac{P_{GEN}^{\max}(\omega_{EM})}{\varepsilon_c C_{11}(\omega_{EM})} - \frac{C_{21}(\omega_{EM})\omega_{EM}}{1000\varepsilon_c C_{11}(\omega_{EM})} - \eta_{tr} split(t) P_{ICE}(t) eng(t) \quad (17)$$

(ii) $split(t) \in [0,1]$ and $split(t)\eta_{tr}P_{ICE}(t)eng(t)$ is a fraction of the engine power while $(1 - split(t)) \cdot \varepsilon_c \cdot \eta_{tr} \cdot P_{ICE}(t) \cdot eng(t)$ is the corresponding fraction of the ICE power delivered to the vehicle path. Note that equations 14 and 16 combine to restrict the mechanical input power to the generator as

$$0 \le P_{GMec} \le \frac{P_{GEN}^{\max}(\omega_{EM})}{C_{11}(\omega_{EM})} - \frac{C_{21}(\omega_{EM})\omega_{EM}}{1000 C_{11}(\omega_{EM})} \quad (18)$$

6. VEHICLE DYNAMICS

To evaluate our controller's velocity tracking performance we consider the longitudinal vehicle dynamics on a flat road. The rate of kinetic energy change in an HEV equals the sum of the internal and external powers acting on the vehicle. As such we represent the vehicle dynamics as a 1st order differential equation in these powers:

$$\dot{V} = -\left(\frac{k_{v1}}{m_c}V^2 + k_{v2}\right) sgn(V) - \frac{1000}{m_c(V+\varepsilon_V)} P_b(t) + \frac{1000\varepsilon_d \varepsilon_c}{m_c(V+\varepsilon_V)} P_F(t) \quad (19)$$

where with v = 0, $P_b(t) = P_{brake}^{\max}(t) \cdot u_{brake}(t)$ (mechanical braking) and $P_F(t) = P_C(t)$ (power from coupling device) whereas with v = 1 $P_b(t) = \frac{1}{\varepsilon_d} P_{reg}^{\max}(t) r(t) + P_{brake}^{\max}(t) u_{brake}(t)$ and $P_F(t) = (1 - split(t))\eta_{tr} P_{ICE}(t) eng(t)$. Note that the first term in equation 19 is aerodynamic drag and rolling resistance losses (power losses), ε_d is the differential efficiency, ε_V is a regularization term, $P_{brake}^{\max}(V)$ is the maximum mechanical braking power, and $u_{brake}(t) \in [0,1]$ is normalized braking control.

To limit the level of maximum braking power at low vehicle velocities for driving comfort, and allow for a high level of braking power at high velocities we set $P_{brake}^{\max}(V) = 50 \cdot \tanh\left(\frac{V}{5}\right)$. Thus summarizing the complete set of HEV dynamical equations at the supervisory level we have:

$$\begin{bmatrix} \dot{P}_{ICE} \\ \dot{\bar{W}}_{bat} \\ \dot{V} \end{bmatrix} = f_{v(t)}\left(\left[P_{ICE},\ \bar{W}_{bat},\ V\right]^{\mathrm{T}}, u_{v(t)}(t)\right) \quad (20)$$

with $u_{v(t)} = \left[u_{ICE}(t),\ eng(t),\ u_{bat}(t),\ u_{brake}(t)\right]^{\mathrm{T}}$ for $v(t) = 0$ and $u_{v(t)} = \left[u_{ICE}(t),\ eng(t), u_{bat}(t),\ u_{brake}(t), split(t), r(t)\right]^{\mathrm{T}}$, for $v(t) = 1$.

7. CONCLUSION

This paper has presented a power flow control model at the supervisory level for an HEV. In part II of this work, this model is utilized in a hybrid optimal control strategy to achieve tracking of a trapezoidal velocity profile over a 12 s. time interval.

8. ACKNOWLEDMENT

We thank Steve Pekarek for many helpful discussions. This work was not supported by NSF or any government agency.

9. REFERENCES

S. Aylor; M. Parten, T. Maxwell and J. Jones "Electrically assisted, hybrid vehicle," *in Proc of IEEE Vehicular Technology Conf,* vol **3**, 1998, pp. 2089.1-2089.6

S. Bengea and R. DeCarlo (2005), "Optimal Control of Switching Systems," *Automatica*, **41**(1), Jan. 2005, pp. 11-27.

A. Brahma, Y. Guezennec and G. Rizzoni (2000), "Dynamic Optimization of Mech/Elec Power Flow in Parallel Hybrid Electric Vehicles," *in Proc the 5th AVEC Int Sym on Advanced Vehicle Control*, Ann Arbor, MI, Aug.

C.C. Chan and K.T. Chau (2001), "Modern Electric Vehicle Technology," Oxford University Press.

M. Cuddy and K. Wipke, "Analysis of the Fuel Economy Benefit of Drivetrain Hybridization," *SAE Paper No. 970289.*

M. Hopka, A. Brahma, S. Dilmi, G. Ercole, C. Hubert, S. Huseman, H, Kim, G. Paganelli, M. Tateno, Y. Guezennec, G. Rizzoni and G. Washington (2001), "The 2000 Ohio State University FutureTruck," *SAE paper.*

C.C. Lin, H. Peng, J.W. Grizzle and J.M. Kang (2003), "Power Management Strategy for a Parallel Hybrid Electric Truck," *IEEE Trans on CST,* **11**(6), Nov, pp. 839-849.

G. Paganelli, M. Tateno, A. Brahma, G. Rizzoni, and Y. Guezennec (2001), "Control development for a hybrid-electric sport-utility vehicle: strategy, implementation and field test results," *in Proc. of the ACC,* Arlington, VA, pp. 5064-5059.

A. Phillips, M. Jankovic, K. Bailey, (2000), "Vehicle system controller design for a hybrid electric vehicle," *in Proc of the IEEE Int Conf on Control App,* Anchorage, AK, USA.

B. Powell, K. Bailey, and S. Cikanek (1998) , "Dynamic modeling and control of hybrid electric vehicle powertrain systems," *IEEE Control Systems Magazine,* **18**(5), pp 17-22.

R. Saeks, C. Cox, J. Neidhoefer, P. Mays and J. Murray (2002), "Adaptive control of a hybrid electric vehicle," *IEEE Transactions on Intelligent Transportation Systems,* **3**(4), pp. 213-234.

K. Uthaichana, S. Bengea, and R. DeCarlo (2005), "Suboptimal supervisory level power flow control of a hybrid electric vehicle," *in Proc of 2005 IFAC World Congress*, Prague, July (to appear)

V. Wouk, "Hybrids: then and now," *IEEE Spectrum*, **32**(7), July 1995, p 16-21